Nonlinear Finite Element Analysis of Reinforced Concrete Shells

Dr.Mustafa K. Kasim   **Ala'a T. Ahmed**   **Abdul-Rahman E. Ibrahim**
Assistant Professor   **Assistant Lecturer**   **Assistant Lecturer**
Civil Eng. Dept.- University of Tikrit

Abstract

This investigation is to develop a numerical model suitable for nonlinear analysis of reinforced concrete shells. A nine-node Lagrangian element Figure (1) with enhanced shear interpolation will be used in this study. Table (1) describes shape functions and their derivatives of this element.

An assumed transverse shear strain is used in the formulation of this element to overcome shear locking. Degenerated quadratic thick plate elements employing a layered discrelization through the thickness will be adopted. Different numbers of layers for different thickness can be used per element. A number of layers between (6 and 10) have proved to be appropriate to represent the nonlinear material behavior in structures. In this research 8 layers will be adequate.

Material nonlinearities due to cracking of concrete, plastic flow or crushing of concrete in compression and yield condition of reinforcing steel are considered. The maximum tensile strength is used as a criterion for crack initiation. Attention is given to the tension stiffening phenomenon and the degrading effect of cracking on the compressive and shear strength of concrete. Perfect bond between concrete and steel is assumed. Attention is given also to geometric nonlinearities. An example have been chosen in order to demonstrate the suitability of the models by comparing the predicted behaviour with the experimental results for shell exhibiting various modes of failure.

Keywords: Finite elements, Nonlinear analysis, Assumed strain, Reinforced concrete shells.

<div dir="rtl">

التحليل اللاخطي باستخدام العناصر المحددة للقشريات الكونكريتية المسلحة

الخلاصة

اجريت هذه الدراسة لغرض الحصول على حل عددي ملائم للقشريات الكونكريتية المسلحة باستخدام التحليل اللاخطي حيث استخدمت عناصر لاكرانج ذات تسعة عقد والتي لها القابلية على تشوه القص لإجراء الحل العددي.

اعتمد انفعال القص المفروض في المعادلات لتجنب حالة القفل بالقص. كذلك استخدمت العناصر الصفائحية المتلاشية رباعية الشكل والسميكة والمرتبة في ثمان طبقات خلال السمك. درس ايضا" التصرف اللاخطي للمادة اعتمادا" على تشقق الكونكريت والجريان اللدن وحالة السحق للخرسانة عند الانضغاط وحالة الخضوع لحديد التسليح. اعلى قيمة لمقاومة الشد اعتمدت كمؤشر لبداية التشقق في الكونكريت.

اعطي الاهتمام ايضا" لحالة مقاومة تصلد الشد للخرسانة المتشققة واخذت ايضا" بنظر الاعتبار مقاومة الانضغاط والقص بعد التشقق. فرض الارتباط التام بين الكونكريت وحديد التسليح . كذلك تمت دراسة التصرف اللاخطي للشكل الهندسي.   تم حل مثال عددي أظهر نتائج ذات توافق جيد مع النتائج العملية كذلك تمت دراسة تأثير انخفاض مقاومة الشد للكونكريت.

الكلمات الدالة:عناصر محددة ، تحليل لاخطي ، إنفعال مفروض ، قشريات كونكريتية مسلحة

</div>

K   Stiffness matrix.

Mx , My , Mxy   Generalized stress components (moments).

N   Shape function.

Q_x , Q_y Generalized stress components (shear forces).

Ri   Shape function.

Si   Shape function.

u,v,w   Displacement components.

ε_x Strain in x-direction.

ε_y Strain in y-direction.

ε_b Bending strain tensor.

ε_s Transverse shear strain tensor.

$\varepsilon_\circ$ Compressive strain at peak stress of concrete.

ε_u Crushing strain.

Notation

Ae   Element area

B   Strain-displacement matrix.

D   Elasticity matrix.

di   Displacement.

E   Young's modulus.

Ec   Initial modulus of elasticity of concrete

Es   Modulus of elasticity of steel

Es'   Second modulus of elasticity of steel.

fc'   Uniaxial compressive strength of concrete.

fc'max   Maximum compressive strength in the direction parallel to the crack direction.

ft '   Uniaxial tensile strength of concrete.

Gc   Fracture energy of concrete.

I1 , J2 Normal and shear stress invariants.

J   Jacobian matrix.

| J | Determinant of the Jacobian matrix.

plates and shells. Both an elastic-perfectly plastic and strain hardening plasticity approach are used to model the compressive behavior of the concrete.

Bathe et al.[4] presented a solution capabilities for two and three dimensional nonlinear finite element analysis of concrete structures.

Hu and Schnobrich[5] used a constitutive model based on a smeared crack representation coupled with the rotating crack approach, to predict the post-cracking behavior of reinforced concrete elements subjected to inplane shear and normal stresses.

Hu and Schnobrich[6] used the plane stress constitutive models under monotonic loading for the nonlinear

Introduction

Shells are one of the most important members of structures, while a shell can take loads normal and tangent to the surface, the load on the shell is resisted by transverse shearing forces and by plane stresses. Thus the shell is a combined structure of plate in bending and plate in plane stress.

Hand et al.[1] are the first to use the layered finite element model for determining the load-deflection history up to failure of reinforced concrete plates and shells with the incremental-variable elasticity technique.

Figueiras and Hinton and Owen [2,3] used the finite element method for the nonlinear analysis of reinforced concrete

$$\begin{Bmatrix} u \\ v \\ w \end{Bmatrix} = \sum_{i=1}^{n} \begin{bmatrix} N_i & 0 & 0 & N_i\zeta\dfrac{h_i}{2}l_{1i} & -N_i\zeta\dfrac{h_i}{2}l_{2i} \\ 0 & N_i & 0 & N_i\zeta\dfrac{h_i}{2}m_{1i} & -N_i\zeta\dfrac{h_i}{2}m_{2i} \\ 0 & 0 & N_i & N_i\zeta\dfrac{h_i}{2}n_{1i} & -N_i\zeta\dfrac{h_i}{2}n_{2i} \end{bmatrix} \begin{Bmatrix} u_i \\ v_i \\ w_i \\ \alpha_i \\ \beta_i \end{Bmatrix}$$

…………………………………………..(1)

or simply

$$[U] = \sum_{i=1}^{n} [N_i]\{\delta_i\}$$

……………(2)

Strains at any Gauss point along the thickness (ζ = constant) are defined in the local Cartesian coordinate system (X', Y', Z') by

$$\{\varepsilon\} = \begin{Bmatrix} \varepsilon_{X'} \\ \varepsilon_{Y'} \\ \gamma_{X'Y'} \\ \gamma_{XZ'} \\ \gamma_{YZ'} \end{Bmatrix} = \begin{Bmatrix} \dfrac{\partial u'}{\partial X'} \\ \dfrac{\partial v'}{\partial Y'} \\ \dfrac{\partial u'}{\partial Y'} + \dfrac{\partial v'}{\partial X'} \\ \dfrac{\partial u'}{\partial Z'} + \dfrac{\partial w'}{\partial X'} \\ \dfrac{\partial v'}{\partial Z'} + \dfrac{\partial w'}{\partial Y'} \end{Bmatrix} \quad ………(3)$$

where u', v' and w' are the displacement components in the local system, and their derivatives with respect to the local axes are computed from the global derivatives of the displacement u, v and w in the global coordinate system as:

$$\begin{Bmatrix} \dfrac{\partial u'}{\partial x'} & \dfrac{\partial v'}{\partial x'} & \dfrac{\partial w'}{\partial x'} \\ \dfrac{\partial u'}{\partial y'} & \dfrac{\partial v'}{\partial y'} & \dfrac{\partial w'}{\partial y'} \\ \dfrac{\partial u'}{\partial z'} & \dfrac{\partial v'}{\partial z'} & \dfrac{\partial w'}{\partial z'} \end{Bmatrix} = [\Omega]^T \begin{Bmatrix} \dfrac{\partial u}{\partial x} & \dfrac{\partial v}{\partial x} & \dfrac{\partial w}{\partial x} \\ \dfrac{\partial u}{\partial y} & \dfrac{\partial v}{\partial y} & \dfrac{\partial w}{\partial y} \\ \dfrac{\partial u}{\partial z} & \dfrac{\partial v}{\partial z} & \dfrac{\partial w}{\partial z} \end{Bmatrix} [\Omega]$$

……………………………..………..(4)

where $[\Omega]$ is the transformation matrix.

finite element analysis of reinforced concrete structures.

Abbasi et al.[7] used the nonlinear finite element modeling to show the various failure modes of a reinforced concrete slab in terms of damage accumulation either by tension cracking in concrete, plastic yielding in steel or by concrete crushing.

Sathurappan et al.[8] used the finite element method in its incremental form to analyze the nonlinear problem where both material and geometric nonlinearities are used.

Polak and Vecchio[9] developed a heterosis-type degenerate isoparametric quadrilateral element by using a layered-element formulation for the analysis of reinforced concrete shell structures. They used selective integration to avoid shear locking and zero energy problems.

Abdullah[10] studied the influence of tension stiffening models on geometric and material nonlinear analysis of reinforced concrete shells. A nine-node Lagrangian degenerate element has been employed.

The present study will use the finite element method for analyzing the nonlinear behavior of reinforced concrete shells comparing the effect of varies failure criterions for concrete.

Basic Theory

Using the degenerated shell element, the global displacements at any point (ξ, η, ζ) in the element field can be expressed in terms of the nodal displacements as

The stiffness matrix is computed by summing up the contribution of each layer stresses at the Gauss points

$$[K^e] = \sum_{Lay.} \int_{Vol} [B]^T [D][B] J \, dVol \quad \ldots\ldots\ldots(8)$$

The internal force vector (or equivalent nodal forces) at the end of each iteration are defined by

$$[f^e] = \sum_{Lay.} \int_{Vol} [B]^T [\sigma] J \, dVol$$

$$\ldots\ldots\ldots\ldots\ldots\ldots\ldots\ldots\ldots\ldots(9)$$

Assumed Transverse Shear Strain Fields

A new shear strain field is to be interpolated from the strain values at the sampling points for the elimination of shear locking. This displacement field is used to evaluate $(\gamma_{\xi\zeta})$ and $(\gamma_{\eta\zeta})$ which are the transverse shear strains as:

$$\gamma'_{\xi\zeta} = \sum_{i=1}^{n} R_i(\xi,\eta)\gamma^i \xi\zeta \quad \ldots\ldots\ldots(10)$$

$$\gamma'_{\eta\zeta} = \sum_{i=1}^{n} S_i(\xi,\eta)\gamma^i \xi\zeta \quad \ldots\ldots\ldots(11)$$

where $(\gamma'_{\xi\zeta})$ and $(\gamma'_{\eta\zeta})$ are the transverse shear strain at certain sampling points (i) while (R_i) and (S_i) are the appropriate shape functions.
Thus the shear strain can be expressed [11] as:

$$\begin{Bmatrix} \gamma'_{\xi\zeta} \\ \gamma'_{\eta\zeta} \end{Bmatrix} = L \begin{Bmatrix} \gamma'_{xz} \\ \gamma'_{yz} \end{Bmatrix} \quad \ldots\ldots\ldots\ldots(12)$$

in which

$$L = \frac{\partial z}{\partial \zeta} \begin{bmatrix} \partial x/\partial\xi & \partial y/\partial\xi \\ \partial x/\partial\eta & \partial y/\partial\eta \end{bmatrix} = \frac{h}{2} J$$

$$\ldots\ldots\ldots\ldots\ldots\ldots\ldots\ldots\ldots..(13)$$

The derivatives of the global displacements with respect to the global coordinates may be expressed in the usual manner as:

$$\begin{Bmatrix} \dfrac{\partial u}{\partial x} & \dfrac{\partial v}{\partial x} & \dfrac{\partial w}{\partial x} \\ \dfrac{\partial u}{\partial y} & \dfrac{\partial v}{\partial y} & \dfrac{\partial w}{\partial y} \\ \dfrac{\partial u}{\partial z} & \dfrac{\partial v}{\partial z} & \dfrac{\partial w}{\partial z} \end{Bmatrix} = [J]^{-1} \begin{Bmatrix} \dfrac{\partial u}{\partial \xi} & \dfrac{\partial v}{\partial \xi} & \dfrac{\partial w}{\partial \xi} \\ \dfrac{\partial u}{\partial \eta} & \dfrac{\partial v}{\partial \eta} & \dfrac{\partial w}{\partial \eta} \\ \dfrac{\partial u}{\partial \zeta} & \dfrac{\partial v}{\partial \zeta} & \dfrac{\partial w}{\partial \zeta} \end{Bmatrix}$$

$$\ldots\ldots\ldots\ldots\ldots\ldots\ldots\ldots\ldots\ldots.(5)$$

where $[J]$ is the Jacobian matrix

$$[J] = \begin{Bmatrix} \dfrac{\partial x}{\partial \xi} & \dfrac{\partial y}{\partial \xi} & \dfrac{\partial z}{\partial \xi} \\ \dfrac{\partial x}{\partial \eta} & \dfrac{\partial y}{\partial \eta} & \dfrac{\partial z}{\partial \eta} \\ \dfrac{\partial x}{\partial \zeta} & \dfrac{\partial y}{\partial \zeta} & \dfrac{\partial z}{\partial \zeta} \end{Bmatrix}$$

$$\ldots\ldots\ldots\ldots\ldots\ldots\ldots..\ldots\ldots(6)$$

The five stress components in the local coordinates system are:

$$\{\sigma\} = \begin{Bmatrix} \sigma_{X'} \\ \sigma_{Y'} \\ \tau_{X'Y'} \\ \tau_{X'Z'} \\ \tau_{Y'Z'} \end{Bmatrix} = [D](\{\varepsilon\} - \{\varepsilon_0\})$$

$$\ldots\ldots\ldots\ldots\ldots\ldots\ldots\ldots\ldots.(7)$$

where $\{\varepsilon_0\}$ may represent any initial strains such as the expansion due to thermal load.

The moment-curvature and shear force–shear strain relations can be written as:

$$[M_x, M_y, M_{xy}]^T = D_b \varepsilon_b \ldots\ldots\ldots(18)$$

$$[Q_x, Q_y]^T = D_s \varepsilon_s' \ldots\ldots\ldots\ldots(19)$$

Considering (K_{ij}') as the stiffness matrix coefficients at node (i) and (j) which represent bending and transverse shear strain energy and by using full integration rule in $(\xi - \eta)$ direction then the function for bending:

$$K_{f_{ij}}^e = \int_{A_e} B_{f_i}^T D_f B_{f_j} \, dA \ .\ldots\ldots\ldots(20)$$

And for shear:

$$K_{s_{ij}}^{'e} = \int_{A_e} B_{s_i}'^T D_s B_{s_j}' \, dA \ \ldots\ldots\ldots..(21)$$

where (A_e) is the element area

Material Modeling
Failure Criteria for Concrete

The strength of concrete under multiaxial stress is a function of the state of stress and cannot be predicted by limitation of simple tensile, compressive or shearing stress independently of each other. The general shape of failure surface is defined by the stress invariants I_1, J_2 and J_3, where I_1 is the first stress invariant and J_2 and J_3 are the second and the third invariant of the deviatoric stress tensor.

In the present work, three criteria will be described and used to model the concrete in compression. Comparison between these criterions is discussed through analyzing reinforced concrete members and comparing with the published experimental results.

Generalized Willam Criterion

Menerterey and Willam refined the three-parameter Willam criterion by

and (h) is the thickness and (J) is the Jacobian matrix. It is possible to write the same thing, for :

$$\frac{\partial \xi}{\partial z} = \quad \frac{\partial \eta}{\partial z} \quad = \quad \frac{\partial \zeta}{\partial x} \quad = \quad \frac{\partial \zeta}{\partial y} = \quad 0$$
$$\ldots\ldots\ldots\ldots\ldots\ldots\ldots\ldots...\ldots(14)$$

in which

$$\begin{Bmatrix} \gamma_{xz}' \\ \gamma_{yz}' \end{Bmatrix} = L^{-1} \begin{Bmatrix} \gamma_{\xi\zeta}' \\ \gamma_{\eta\zeta}' \end{Bmatrix} \ \ldots\ldots\ldots.\ldots(15)$$

while

$$L^{-1} = \frac{2}{h} J^{-1} \ \ldots\ldots\ldots\ldots\ldots.....(16)$$

Using the full integration a shear locking problem will appear. Therefore, reduced integration could be used but there will appear another problem which is zero energy modes. These problems can be solved by using assumed strain elements where ($\gamma_{\xi\zeta}'$) is linear in (ξ) direction to overcome shear locking and quadratic in (η) direction to overcome zero energy modes and ($\gamma_{\eta\xi}'$) is linear in (η) direction and quadratic in (ξ) dire

The strain displacement matrix *B* , in the finite element method, which relates the strain components to the nodal displacements is given in :
equation can be written in partitioned form as:

$$\begin{Bmatrix} \varepsilon_b \\ \varepsilon_s' \end{Bmatrix} = \begin{Bmatrix} \sum_{i=1}^{n} B_{bi} \, d_i \\ \sum_{i=1}^{n} B_{si}' \, d_i \end{Bmatrix} \ \ldots\ldots\ldots..(17)$$

where (ε_b) is the bending strain, (ε_s') is assumed transverse shear strain, (B_s') is the shear strain displacement matrix.

Ottosen Criterion

Ottosen suggested a four-parameter criterion[16]. The failure surface has curved meridians and noncircular cross sections. The failure curves on the deviatoric plan change from nearly triangular to the nearly circular with increasing hydrostatic pressure and this criterion can be represented by:

$$f(I_1, J_2, \cos 3\theta) = a\frac{J_2}{f_c^{'2}} + \lambda_f \frac{\sqrt{J_2}}{f_c^{'}} + b\frac{I_1}{f_c^{'}} - 1$$

....(28)

$$\lambda_f = k_1 \cos\left[\frac{\Pi}{3} - \frac{1}{3}\cos^{-1}(-k_2\cos 3\theta)\right]$$

for $\cos 3\theta \leq 0$ ....(29)

$$\lambda_f = k_1 \cos\left[\frac{1}{3}\cos^{-1}(k_2\cos 3\theta)\right]$$

for $\cos 3\theta \geq 0$ ....(30)

I_1: is the first stress invariant tensor $\left(I_1 = v_1 + v_2 + v_3 = \sigma_x + \sigma_y + \sigma_z\right)$

J_2: is the second invariant of stress deviatoric tensor.

k_1, k_2, a, b are material parameters.

The four parameters in the failure criterion are determined on the basis of two typical uniaxial concrete tests ($f_c^{'}$ and $f_t^{'}$) and two typical biaxial and triaxial concrete data.

In the present study, the four-parameter criterion which agrees well with experimental results[17] are adopted as
   a = 0.9218, b = 2.5969, k₁ = 9.9110,
and k₂ = 0.9647.

Figure (5) illustrates the agreement between the Ottosen criterion and the experimental data referred to the compressive and tensile meridians. The

adjusting the compression and tension meridians[12]. These meridians are no longer straight lines. The adjustment also is made to the deviatoric plane which depends on the eccentricity (e).

$$f(\xi_f, \rho_f, \theta) = \left[\sqrt{1.5}\frac{\rho_f}{f_c^{'}}\right]^2 + m\left[\frac{\rho_f}{\sqrt{6}f_c^{'}}r(\theta,e) + \frac{\xi_f}{\sqrt{3}f_c^{'}}\right] - 1 = 0$$

....(22)

$$r(\theta,e) = \frac{4(1-e^2)\cos^2\theta + (2e-1)^2}{2(1-e^2)\cos\theta + (2e-1)\left[4(1-e^2)\cos^2\theta + 5e^2 - 4e\right]^{0.5}}$$

....(23)

$$\xi_f = \tfrac{1}{3}I_1$$ ....(24)

$$\rho_f = \sqrt{2J_2}$$ ....(25)

$$\cos 3\theta = \frac{3\sqrt{3}}{2}\frac{J_3}{J_2^{\frac{3}{2}}}$$ ....(26)

$$m = \frac{(f_c^{'})^2 - (f_c^{'})^2}{f_c^{'}f_1^{'}}\frac{e}{e+1}$$ ....(27)

The eccentricity value e is obtained from a figure which depends on the relation between the axial and biaxial compressive strength $\frac{f_{bc.}^{'}}{f_c^{'}}$ and also on the relation of uniaxial compressive strength and uniaxial tensile strength relation $\frac{f_t^{'}}{f_c^{'}}$ [13]. For example e = 0.52 is obtained by using $\frac{f_{bc.}^{'}}{f_c^{'}} = 1.14$ and $\frac{f_t^{'}}{f_c^{'}} = 0.1$ which give good agreement when compared with the experimental results of Kupfer et al. [13], Figure (4) in the deviatoric plan. The comparison of this criterion in the meridian plan for compression and extension meridian gives good agreement with triaxial test data by Chinn and Zemmerman [14] and Mill and Zemmerman [15] Figure(3).

carries, between cracks, a certain amount of tensile stress normal to the cracked plane. The concrete between cracks adheres to the reinforcing bars and contributes to the overall stiffening of the structure. The strain softening or descending branch of the stress strain curve of concrete in tension, in one form or another, may be used to simulate this "tension stiffening" effect. After cracking, the tension carried by the concrete is calculated as the net area of concrete times the average tensile stress in the concrete between the cracks.

Tension Stiffening (Parabolic Model)

When the finite element is used in the analysis of reinforced concrete structures, it has been found that the overall stiffness and predicted ultimate load decrease with the reduction of element number[8]. The cracking model exhibits greater softening when the number of elements increase. Fracture energy (G_c) is applied to overcome this difficulty and to relate the constitutive model to objective measures.

This fracture energy is defined as the amount of energy required to create a crack of one unit of area, sometimes (G_c) called the critical strain energy release rate or toughness.

The relationship between stress and strain after cracking is given in Figure(7)[11] :

$$\sigma = f_t^{©} \left(\frac{\varepsilon_1 - \varepsilon_m}{\varepsilon_t - \varepsilon_m}\right)^2 \dots\dots\dots\dots\dots(33)$$

where $(f_t^{©})$ is the tensile strength and (ε_t) is tensile strain at maximum tensile stress. In the analysis of the two

ability of this criterion to represent the experimental biaxial data of Kupfer et. al [13] is shown in Figure (6).

Compressive Behavior of Concrete

Based on the flow theory of plasticity, the nonlinear compressive behavior of concrete is modeled. Adopting Kupfer's results[13], the yield condition for the slab can be written in term of the stress components as [3]:

$$f(\sigma) = \left\{1.355\left[(\sigma_x^2 + \sigma_y^2 - \sigma_x\sigma_y) + 3(\tau_{xy}^2 + \tau_{xz}^2 + \tau_{yz}^2)\right] + 0.355\sigma_o(\sigma_x + \sigma_y)\right\}^{0.5} = \sigma_o$$

..………………………………....(31)

where (σ_o) is the equivalent effective stress taken as the compressive strength $(f_c^{'})$ which is obtained from uniaxial test.

Both perfectly plastic and strain hardening models are represented in one-dimensional form in Figure (2).

The crushing of concrete is a strain control phenomenon. A simple way of incorporation in the model is to convert the yield criterion of stresses directly into the strains, and the crushing condition can be expressed in terms of the total strain components as:

$$\left\{1.355\left[(\varepsilon_x^2 + \varepsilon_y^2 - \varepsilon_x\varepsilon_y) + 0.75(\gamma_{xy}^2 + \gamma_{xz}^2 + \gamma_{yz}^2)\right] + 0.355\varepsilon_o(\varepsilon_x + \varepsilon_y)\right\}^{0.5} = \varepsilon_o^2$$

………………………………....(32)

The concrete is assumed to lose all its characteristics of strength and rigidity when (ε_u) reaches the specified ultimate strain.

The response of concrete in tension is assumed to be as Tension stiffening, illustrates that the cracked reinforced concrete as a result of bond mechanisms

primary variables in the shear transfer mechanism as indicated in experimental work. The amount of shear stress can be transferred across the rough surfaces of a cracked concrete, and the dowel action of steel is contributing to the shear stiffness across the cracks[18]. An appropriate value of the cracked shear modulus can be estimated in a smeared cracking model[19,20]. In the present study, the cracked shear modulus is assumed to be a function of the current tensile strain. In this approach a value of (G') linearly decreasing with the current tensile strain is adopted by Cedolin and Deipoli[18] and used by many investigators[3] .

For concrete cracked in direction 1.

$$G'_{12} = 0.25G(1 - \varepsilon_1 / 0.004)$$

for $\varepsilon_1 < 0.004$

$$G'_{12} = 0$$

for $\varepsilon_1 > 0.004$

$$G'_{13} = G'_{12}$$

$$G'_{23} = \frac{5}{6}G$$

…………….....(38)

where (G) is the uncracked shear modulus and (ε_1) is the tensile strain in direction 1. For concrete cracked in both directions:

$$G'_{13} = 0.25G(1 - \varepsilon_1 / 0.004)$$

for $\varepsilon_1 < 0.004$

$$G'_{13} = 0$$

for $\varepsilon_1 > 0.004$

$$G'_{23} = 0.25G(1 - \varepsilon_2 / 0.004)$$

for $\varepsilon_2 < 0.004$

$$G'_{23} = 0$$

for $\varepsilon_2 > 0.004$

dimensional problems, a parabolic curve is used to simulate the relationship between stress and strain after cracking (based on fracture energy value) see Figure (7).

The fracture energy corresponding to an opening crack can be evaluated as[11]:

$$G_c = \int_{\varepsilon_t}^{\varepsilon_m} \sigma \, h_c \, d\varepsilon \quad …….…………..…(34)$$

Solving the integration gives:

$$G_c = \frac{h_c \, f_t^{©}(\varepsilon_m - \varepsilon_t)}{3} \quad …..………..…..(35)$$

The maximum tensile strain (ε_m) can be evaluated from equation (35) as:

$$\varepsilon_m = \frac{3G_c}{h_c \, f_t^{©}} + \varepsilon_t …………………..…(36)$$

where (G_c) is the fracture energy of concrete. The value for normal aggregate concrete seems to be (60-100)N/m [3] has stated that for normal concrete, typical values for (G_c) lie in the range $(200 f_t^{©2} / E_c)$ to $(400 f_t^{©2} / E_c)$. In the present study (G_c) is taken equal to 100 N /m.

(h_c) is the characteristic length of the Gauss point, and is equal to:

$$h_c = \sqrt{(dA)} …….…..…………………(37)$$

where (dA) is the area represented by the Gauss point.

Cracked Shear Modulus

The crack width, aggregate size, reinforcement ratio and bar size, are the

following formula are describe the geometrical nonlinearity by the degenerated elements using the tangential stiffness matrix method to obtain the geometric stiffness matrix which can be written as:

$$[K]_\sigma = \int_V [G]^T \{\sigma\}[G]dv \dots\dots\dots\dots(41)$$

in which the term $[G]$ is a geometric matrix with two rows and a number of columns equal to the total number of element nodal variables. The first row contains the contribution of each nodal variable to the local derivative $\dfrac{\partial w'}{\partial x'}$ (corresponding shape function derivatives) and the second row contains the contributions for $\dfrac{\partial w'}{\partial y'}$ and $\{\sigma\}$ is the components of the stress vector defined previously from Equation (7).

Numerical Examples
Example 1

The parabolic cylindrical shell tested by Hedgren existing in [4] is analyzed. This is supported on end diaphragms and has free longitudinal edges with variable thickness. The shell is subjected to uniformly distributed pressure with ultimate value of (0.01435) MPa. The shell geometry is shown in Fig. (8-a) and (8-b) finite elements are used to model one quarter of the shell, each of which is divided into (8) equal concrete layers. Concrete properties and reinforcement characteristics are given in Tables (2) and (3).The resulting load- deflection curves at the crown of the mid-span section show the following:

$$G'_{12} = 0.5G'_{23}$$

for $G'_{23} < G'_{13}$

$$\dots\dots\dots\dots\dots\dots\dots\dots\dots\dots(39)$$

When solving nonlinear problems, the linearization makes it necessary to perform iterative correction to Δd. A Newton-Raphson type scheme is used in this work [3].

Nonlinear Solution

The fundamental approach of the solution for a simple linear elastic problem is generally done by solving a set of equilibrium equations for the unknown displacements $\{a\}$ of the following form:

$$Ka = P \quad or \quad [k]\{a\} = \{p\} \dots\dots\dots\dots(40)$$

A direct solution is not possible in nonlinear problems since the stiffness matrix K depends on the displacement level $K = K(a)$, therefore, it cannot be exactly computed before the determination of the unknown displacement vector a. Either an incremental method, an iterative method or a combination of them is usually used for the solution of nonlinear problems.

An incremental solution procedure with an iterative method has been used to trace out the entire structural response of reinforced concrete structures which dissipate residual forces. The stiffness matrix is computed at stages with a load increment when the change of material characteristics implies a local change of stiffness. During the first spread of cracks and near the ultimate load the stiffness has to be repeatedly calculated.

Geometric Nonlinear Analysis

The causes of structural nonlinearities may be broadly classified in two groups; those from material and geometrical nonlinearities. The material nonlinear behavior has been dealt with before. The

4. Reduction in uniaxial tensile strength of concrete effects to overall strength of reinforced concrete shells.

References

1- Ibrahim, A.E., "Nonlinear Analysis of Reinforced Concrete Plates and Shells Using Assumed Strain Elements" ,M.Sc. Thesis, Tikrit University, 2006.

2- Hand, F.R., Pecknold, D.V. and Schnobrich, W.C., "Nonlinear Layered Analysis of Reinforced Concrete Plates and Shells", Journal of the Structural Division, ASCE, Vol. 99, No. ST7, July 1973, pp. 1491-1505.

3- Figueiras, J.A., "Practical Approach for Modeling the Nonlinear Response of Reinforced Concrete Shells", in Computational Modeling of Reinforced Concrete Structures, edited by E. Hinton and R. Owen, Pineridge Press, Swansea, 1986.

4- Hinton, E. and Owen, D.R.J., "Finite Element Software for Plates and Shells" Pineridge Press, Swansea, 1984.

5- Bathe, K.J. and Bolourchi, S., "A Geometrical and Material Nonlinear Plate and Shell Elements", Journal of Computers and Structures Vol.1l, 1980, pp. 23-48 .

6- Hu, H.T. and Schnobrich, W.C., "Nonlinear Analysis of Cracked Reinforced Concrete", ACI Structural Journal, Vol. 87, No. 2, March- April 1990, pp. 199-207.

7- Hu, H.T. and Schnobrich, W.C., "Nonlinear Finite Element Analysis of Reinforced Concrete Plates and Shells under Monotonic Loading", Journal of Computers and Structures, Vol. 38, No. 5/6,1991, pp. 637-651.

Figure (9) shows the comparison between tension stiffening model with the experimental results. It is found that this model gives a little difference when compared with the experimental results.

Figure (10) shows the effect of different yield criteria. It is found that a little difference exist between the second stress invariant model and the other models.

Figure (11) shows the difference between linear and nonlinear geometry models.

Example 2

This example is same as previous example but with reducing the uniaxial tensile strength of concrete from (4.8) MPa to (4.4) MPa and then to (4.0) MPa. Figure(12) shows the comparison between these values with observed reduction in shells resistance .

Conclusions

Based on the theoretical study presented here, the following specific conclusions can be drawn.

1. The computational models adopted in this study are useful for studying reinforced concrete plates and shells with assumed strain elements based on numerical results obtained in this investigation.

2. The effect of using different yield criteria is studied. It can be concluded that all yield criterion are efficient. The results by using Ottosen and Generalized Willam are similar.

3. Nine-noded element with assumed strain elements to avoid shear locking and tension stiffening models to represent cracked concrete gives good results for the nonlinear analysis of reinforced concrete shell problems.

Under Biaxial Stresses", Proceedings, American Concrete Institute, (ACI), Vol. 66, No. 8, August 1969, pp. 656-666.

15- Chinn,J.and Zimmerman,R.M. (1965)."Behavior of Plain Concrete Under Various High Triaxial Compression Loading Condition" Technical Report,WLTR64-163,New Mexico.

16- Mills, L.L. and Zimmerman, R.M," Compressive Strength of Plain Concrete Under Multiaxial Loading Conditions ", ACI Journal, Vol. 67, No. 10, 1970, pp. 802-807.

17- Ottosen, N.S.,"Failure Criterion for Concrete ". ASCE,Vol., 103,No.EM4.1977.

18- Loo, Y.C. and Guan, H., "Cracking and Punching Shear Failure Analysis of Reinforced Concrete Flat Plates", Journal of Structural Engineering, ASCE, Vol. 12, No. 10, October 1997, pp. 1321-1330.

19- Cedolin, L. and Deipoli, S., "Finite Element Studies of Shear Critical Reinforced Concrete Beams", ASCE Journal of the Engineering Mechanics Division, Vol. 103, No. EM3, June 1977, pp. 395-410.

20- Fenwick, R.C. and Paulay, T., "Mechanics of Shear Resistance of Concrete Beams", ASCE Journal of the Structural Division, Vol. 94, No. ST10, October 1968, pp. 2325-2350.

8- Abbasi, M.S.A., Baluch, M.H., Azad, A.K. and Abdel-Rahman, H.H., "Nonlinear Finite Element Modeling of Failure Modes in Reinforced Concrete Slabs", Journal of Computers and Structures, Vol. 42, No. 5,1992, pp. 815-823.

9- Sathurappan, G., Rajagopalan, N. and Krishnamoorthy, C.S., "Nonlinear Finite Element Analysis of Reinforced Concrete and Prestressed Concrete Slabs with Reinforcement (Inclusive of Prestressing Steel) Modeled As Discrete Integral Component", Journal of Computers and Structures, Vol. 44, No. 3,1992, pp. 575-584.

10- Polak, M.A. and Vecchio, F.J., "Nonlinear Analysis of Reinforced Concrete Shells", Journal of Structural Engineering, ASCE, Vol.119, No. 12, December 1993, pp. 3439-3461.

11- Abdulla, S.M., "Influence of Tension Stiffening Models on Geometric and Material Nonlinear Analysis of Reinforced Concrete Shells", Journal of Eng. and Technology, Mosul University, (Iraq) Vol. 23, No. 10, 2004, pp. 545-562.

12- Abdulla, S.M., "Nonlinear Analysis of Reinforced Concrete Slabs Using Assumed Strain Elements", M.Sc. Thesis, Mosul University, December 1999, 119 pps.

13- Menertrey P.H.,and Willam, K.J"Triaxial Failure Criterion for Concrete and its Generalization" ACI Jornal, Vol. 92, No. 3. (1995).

14- Kupfer, H., Hilsdorf, K.H. and Rush, H., "Behavior of Concrete

Table (1) Shape Functions and Their Derivatives for the Nine-Node Lagrangian Element.

Fun--ction	Corner nodes (1,3,5,7)	Edge nodes (2,6)	Edge nodes (4,8)	Center node (9)
N_i	$\frac{1}{4}(1+\xi_0)(1+\eta_0)(\xi_0+\eta_0-1)$	$\frac{1}{2}(1-\xi^2)(1+\eta_0)$	$\frac{1}{2}(1-\eta^2)(1+\xi_0)$	$(1-\xi^2)(1-\eta^2)$
N_i,ξ	$\frac{\xi_i}{4}(1+\eta_0)(2\xi_0+\eta_0)$	$-\xi(1+\eta_0)$	$\frac{\xi_i}{2}(1-\eta^2)$	$-2\xi_i(1-\eta^2)$
N_i,η	$\frac{\eta_i}{4}(1+\xi_0)(2\eta_0+\xi_0)$	$\frac{\eta_i}{2}(1-\xi^2)$	$-\eta(1+\xi_0)$	$-2\eta_i(1-\xi^2)$

Table (2) Material Properties for Shell.

E_c MPa	f_c' MPa	v_c	f_t' MPa	ε_u	a	ε_m	E_s' MPa	E_s MPa
20690	30.2	0.145	4.8	0.0035	0.6	0.002	0.0	200000

Table (3) Reinforcement Characteristics [N,mm] for Shell.

Designation	Diameter mm	Area mm^2	Yield Strength MPa	Ult. Strength MPa
No. 3	1.22	1.17	225.3	364.2
No. 4	1.57	1.95	221.9	344.5
No. 9	3.43	9.2	307.0	420.0
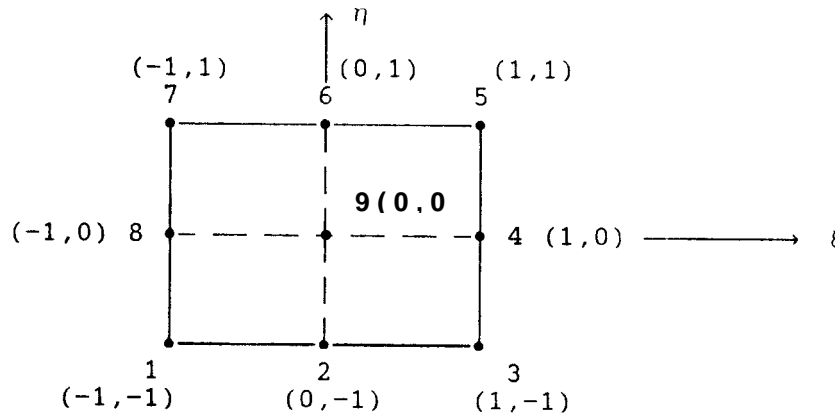
Figure (1) A Nine-Node Lagrangian Element.
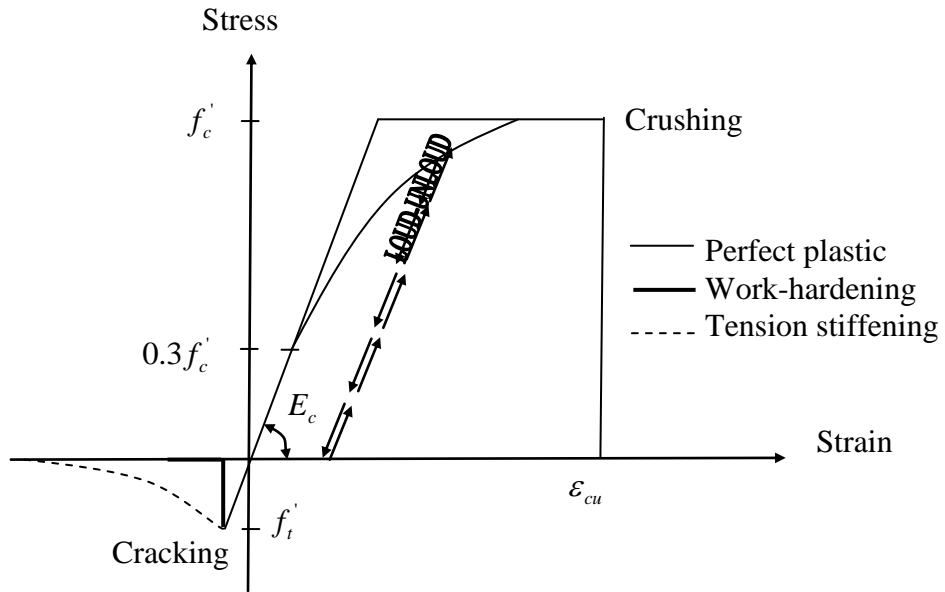
Figure (2) One-dimensional representation of the concrete constitutive model[23].
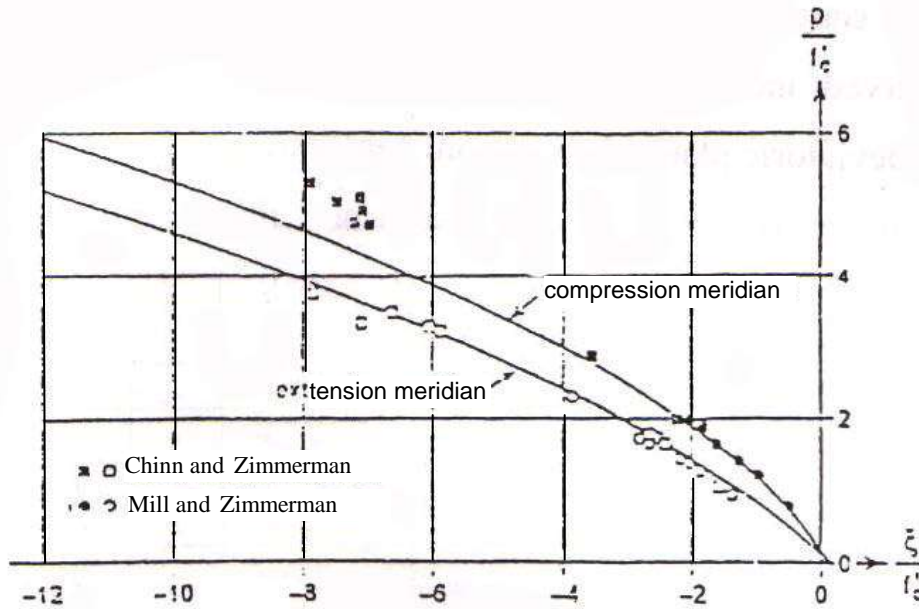
Figure (3) A Comparison of Three-Parameter Concrete Criterion With Triaxial Test Data by Chinn and Zimmerman[15] and Mills and Zimmerman[16].

Envelope of Experimental Results
Concrete failure Criterion
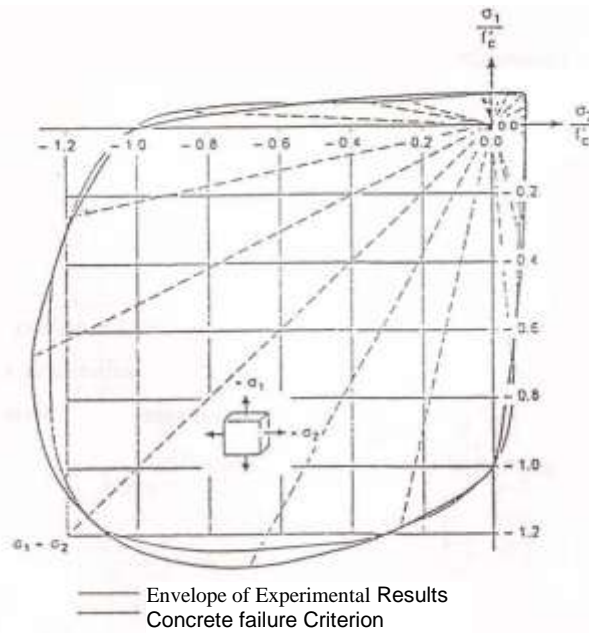
Figure (4) A Comparison of Three-Parameter Concrete Criterion With

Biaxial Test Data by Kupfer et al. [14].
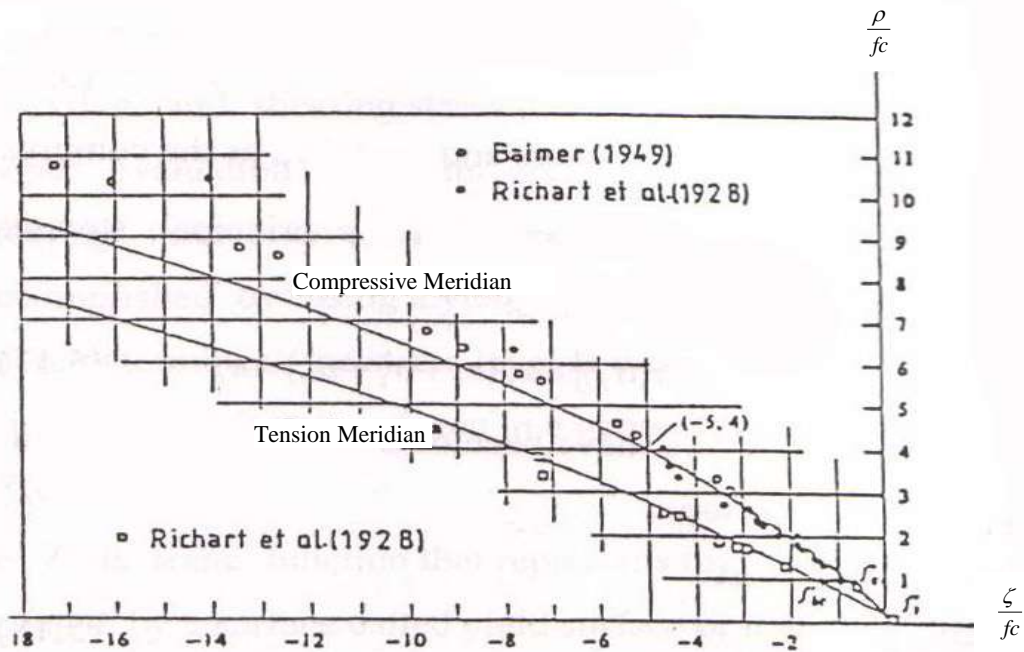
Figure (5)Correlation Between Ottosen Criterion and Experimental Data[17].

$\dfrac{\sigma_1}{fc}$

$\dfrac{\sigma_2}{fc}$

$f_c^{'} = 59.4 MPa$

$f_t^{'} / f_c^{'} = 0.08$

Kupfer et al (1969,1973)

Failure criterion
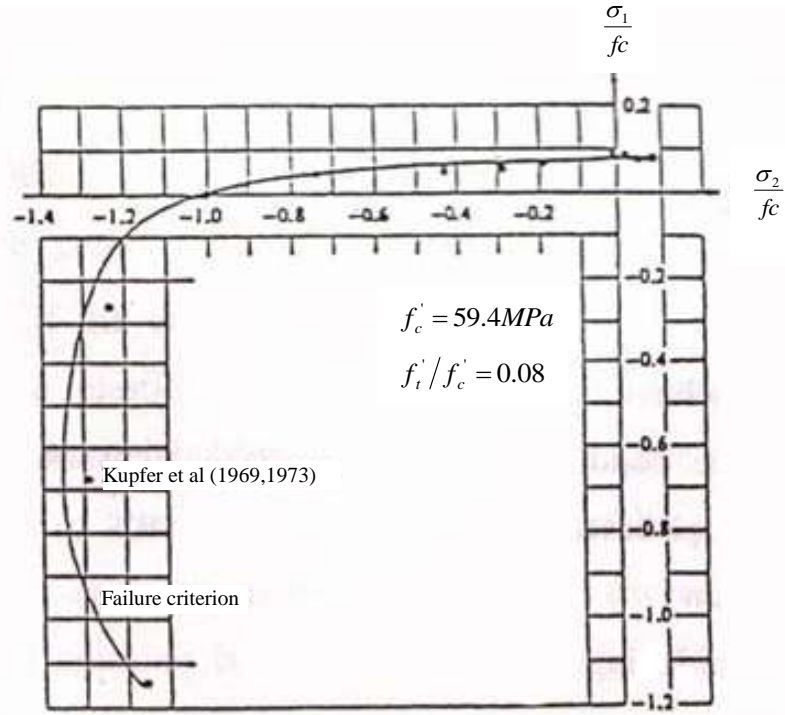
Figure (6) Biaxial Representation for Ottosen Criterion[17].

Stress

$f_t^{'}$

$\sigma = f_t^{'} (\dfrac{\varepsilon_1 - \varepsilon_m}{\varepsilon_t - \varepsilon_m})^2$

ε_{cr}

Strain

ε_m
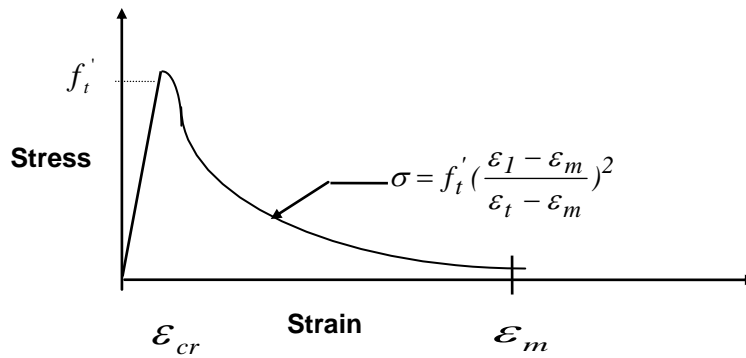
Figure(7) Tension Softening (Parabolic Model).
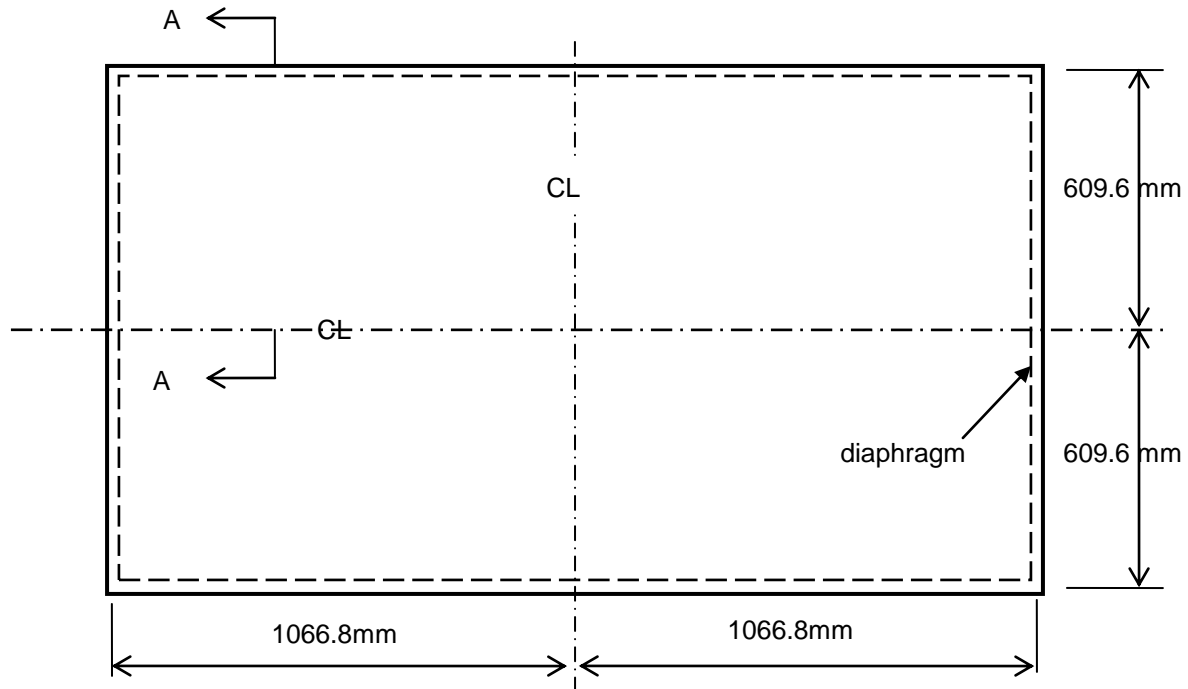
Figure (8-a) Plan of Hedgren Cylindrical Shell[4].
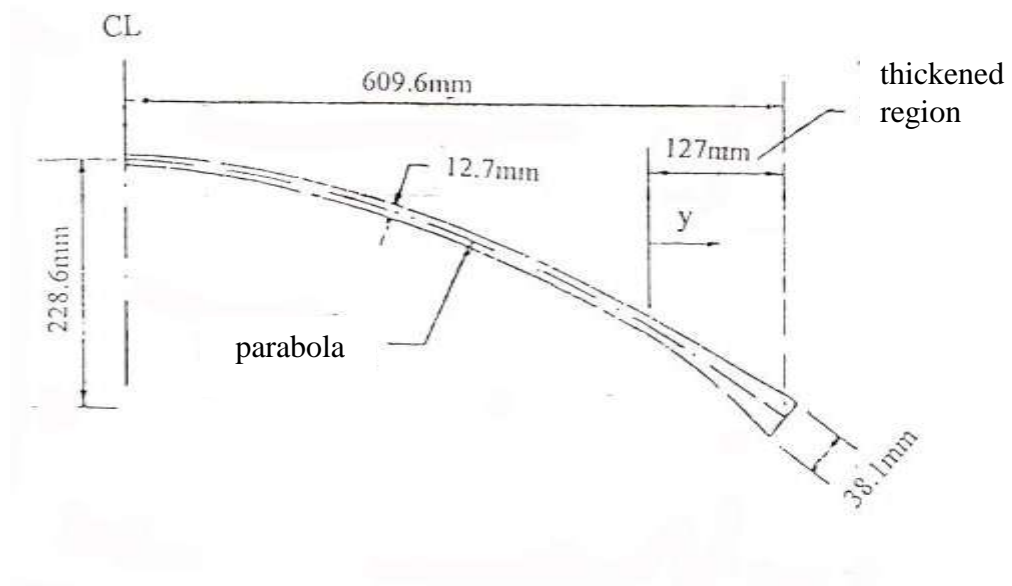
Figure (8-b) Section A-A of Hedgren Cylindrical Shell[4].
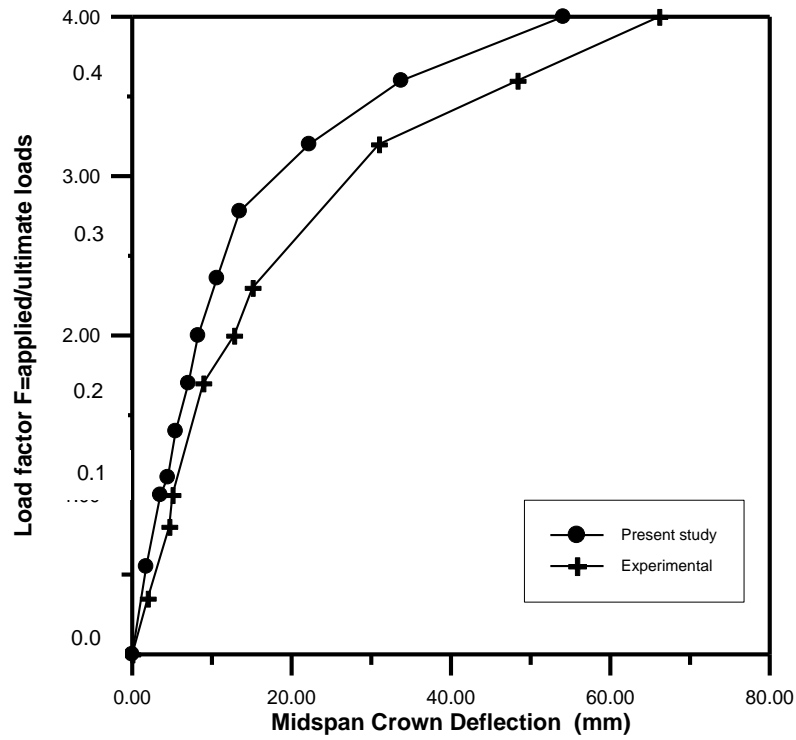
Figure(9) Load-Deflection Curves for Tension Stiffening .
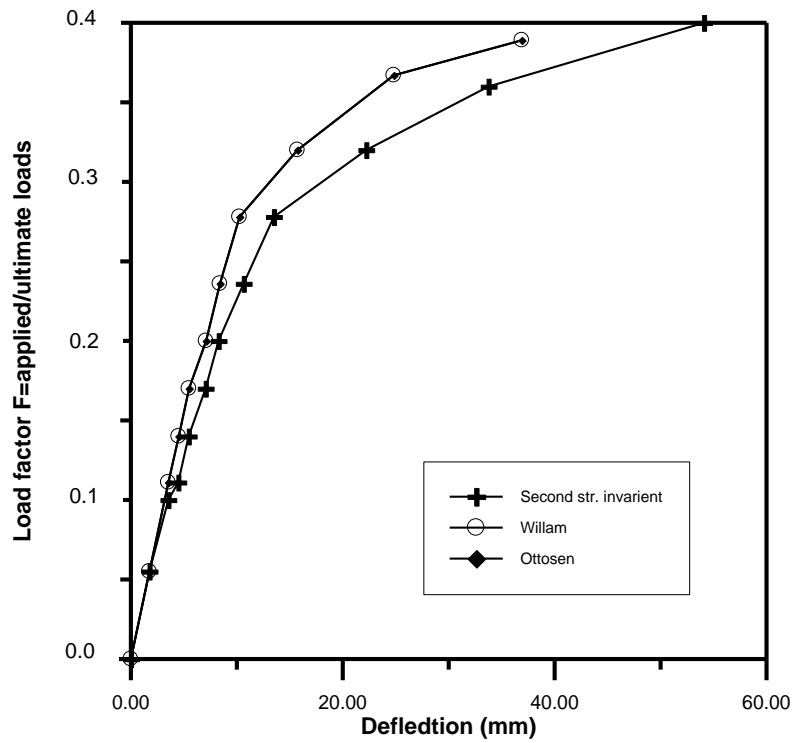
Figure (10) Load-Deflection Curves With Different Yield Criterion.
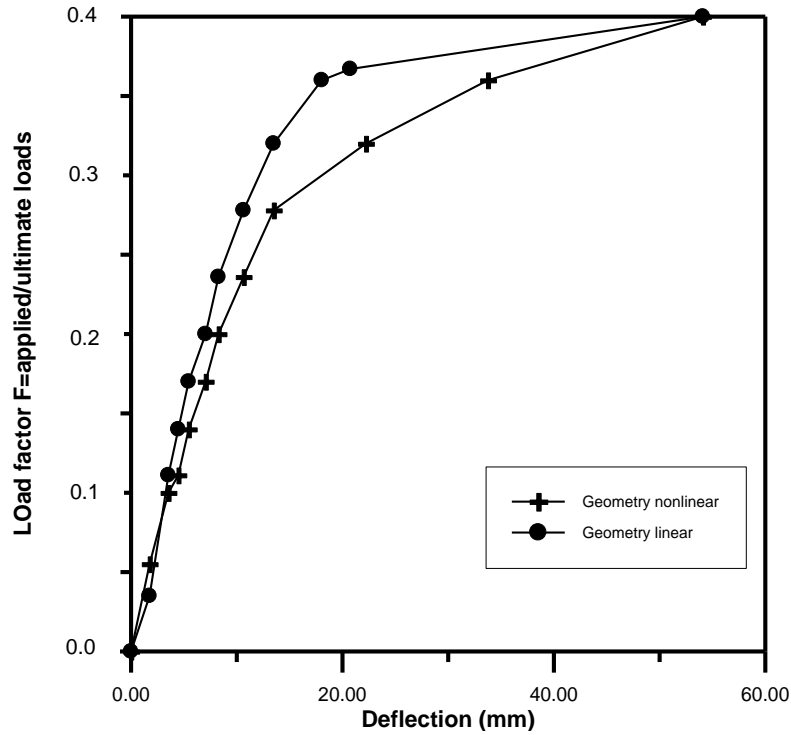
Figure (11) Load-Deflection Curves for Geometric Linear and Geometric Nonlinear.
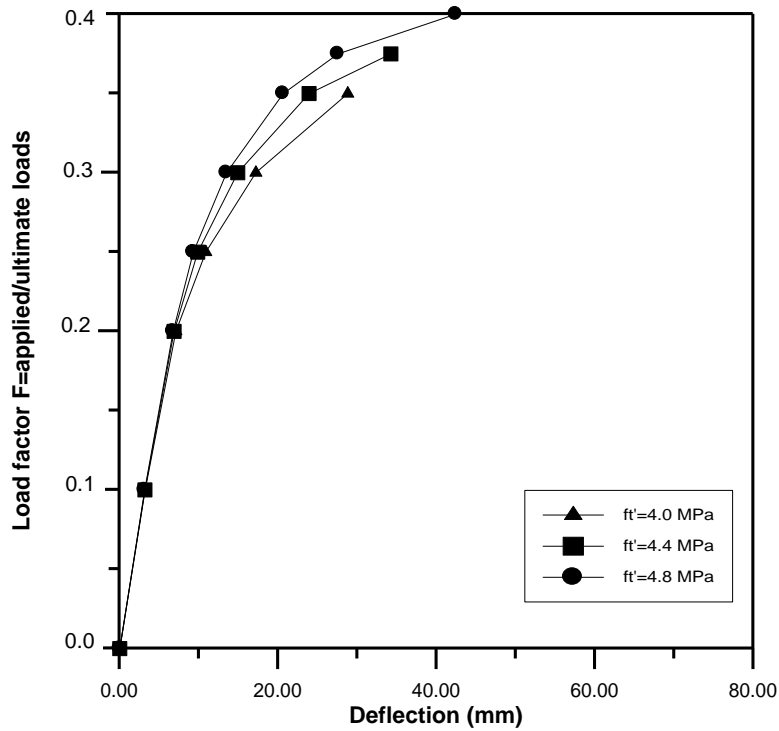
Figure (12) The Effect of Uniaxial Tensile Strength of Concrete